Analysis of Membranless Formic Acid Fuel Cell using E-Shaped Microfluidic Channel

M. Elumalai[1], M. Raja[2], A. Rajasekaran[3] and B. Chinnaraja[4]

[1]Department of Chemistry, School of Basic Science, VISTAS, Pallavaram, Chennai-600117, India
[2]Department of Statistics, Tagore College of Arts and Science, Chrompet, Chennai-600117, India
[3]Department of Chemistry, Dhanalakshmi Srinivasan College of Engineering and Technology, Chennai-603104, India
[4]Department of Public Administration, University of Madras, Chennai-600005, India

*Corresponding author: E-mail: elu.ashwin@gmail.com

A microfluidic fuel cell has been fabricated using formic acid in an alkaline media as the fuel and sodium percarbonate in acidic media as the oxidant. Various operating conditions and different cell dimensions were applied to evaluate the fuel cell performance. The laminar flow-based membraneless fuel cell was found to reach a maximum power density of 23.60 mW cm^{-2} using 1.50 M HCOOH in 3 M NaOH solution as the fuel and 0.15 M percarbonate in 1.50 M H$_2$SO$_4$ solution as the oxidant at room temperature. The fuel cell system has no proton exchange membrane. This simple membraneless fuel cell with a planar structure has a high design flexibility, which enables its easy integration into actual microfluidic systems and miniature power applications.

Keywords: Membraneless, Formic acid, Fuel cell, Miniature power applications, Power density.

INTRODUCTION

A small fuel cell received much attention due to their widely promising application in portable power sources. Among fuel cell systems that are in use, the microfluidic fuel cells have been recognized as one of the most promising candidates for small-scale portable power applications [1-3]. A typical membraneless fuel cell consists of two electrodes placed on the side walls along the channel. In such a system, the fuel and oxidant are passed into the microchannel at a low flow rate, follow-on in a laminar flow. The laminar flow performs the replication of the solid membrane in proton exchange membrane fuel cells and facilitates the separation of fuel and oxidant.

Formic acid seems to be a promising fuel for microfluidic fuel cells, due to high efficiency (Fig. 1) and more hydrogen content than other types of fuel (Fig. 2). The main advantages of formic acid fuel cell are that formic acid is a liquid at room temperature and can easily be stored. Similar to methanol, it has small organic molecules fed directly into fuel cell, removed for the need of complicated catalytic reforming.

The membraneless formic acid fuel cell (MLFAFC) developed in the present study employs an alkaline solution of formic acid as a fuel and an acidic solution of sodium percarbonate (2Na$_2$CO$_3$·3H$_2$O$_2$) as an oxidant. A number of drawbacks associated with membrane cells that were discussed earlier can be avoided in MLFAFCs. Assessing the performance of fuel cell in alkaline and acid media (one electrode is acidic and the other one is alkaline) is the focus of this study. Sodium percarbonate is an environmentally friendly, cost-effective, non-toxic, large-scale industrial chemical used primarily in detergents and as a mild oxidant. It is a true peroxo salt and readily available source of hydrogen peroxide [4,5].

$$2Na_2CO_3·3H_2O_2 \longrightarrow 2Na_2CO_3 + 3H_2O_2 \qquad (1)$$

A unique feature of sodium percarbonate is that it can be used not only as an oxidant but also as a reductant [6,7], which is an advantage compared to fuel cells that use hydrogen peroxide. On the performance side, MLFAFC generates electric power comparable to a typical air-breathing direct methanol fuel cell (DMFC) operating in a microchemical channel at room temperature. These advantages make MLFAFCs a suitable alternative for portable power applications. We have developed a new simplified architecture, which is unique from those that have been reported in the literature, by eliminating and integrating
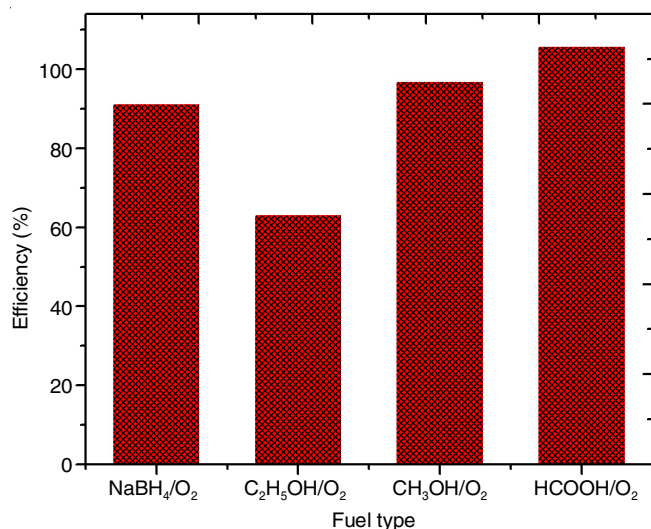
Fig. 1. Efficiency of different types of fuels
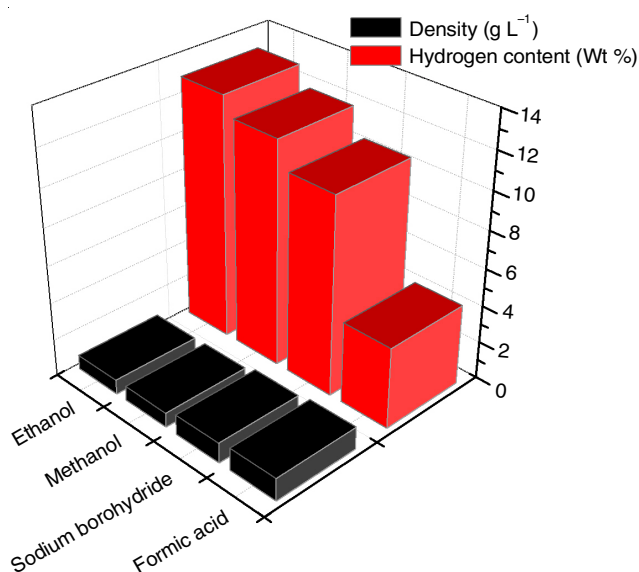
Fig. 2. Hydrogen content and density of various kinds of fuels

the key components of a conventional membrane electrode assembly (MEA) in this study.

The aim of this study is to develop a membraneless microfluidic fuel cell operating in alkaline and acid media. Experimental methods are applied to a planar microfluidic fuel cell design employing platinum-coated carbon electrode as the anode as well as the cathode. In this work, the membraneless formic acid fuel cell is tested in all-acidic, all-alkaline and acid-alkaline media to ascertain the best media configuration for further fuel cell experiments. The effect of variation of fuel and oxidant concentrations, flow rate variations, electrolyte variations and electrode distance were also considered in order to improve the performance of fuel cell.

EXPERIMENTAL

The chemicals handled in the planar membraneless fuel cell design were formic acid (98 %, Merck), NaOH (98 %, Merck), $2Na_2CO_3 \cdot 3H_2O_2$ (99 %, Riedel) and H_2SO_4 (98 %, Merck). All the solutions were prepared in deionized water. The materials used in fuel cells were poly(dimethylsiloxane) (PDMS; 99.9 %,

Chemsworth) and poly(methylmethacrylate) (PMMA; 92 %, G. Khanna & Co.), graphite plates (Kriti Graphite) and silicon tubes (Shree Gaurav Rubber Products).

Catalyst deposition: In MLFAFCs, graphite plates act as current collectors and catalyst structures. For all the experiments of fuel cells, unsupported platinum black nanoparticles are applied to the sides of graphite plates so that they serve as cathode and as anode that line the microfluidic channel. For both electrodes, the catalyst suspensions were prepared by mixing Pt black nanoparticles (Alpha Aesar) at a concentration of 6.0 mg mL^{-1} in a 10 wt.% Nafion solution (Nafion stock solution: Dupont, 5 % (w/w) solution). This mixture was sonicated and hand-painted on to the side faces of graphite plates at a loading of 2 mg cm^{-2}. Then solvent was evaporated by the use of a heat lamp for uniform loading [8].

Formulation of fuel cell: The E-channel structure required for co-laminar flow was moulded with poly(dimethylsiloxane) (PDMS), typically 1-10 mm in thickness, after coating it with 1 mm thick graphite plate. To provide rigidity and robustness to the layered system, more rigid top and bottom capping layers were formed, such as 2 mm poly(methylmethacrylate) (PMMA). To guide the fuel and the oxidant into the E-shaped channel systems and to let the waste stream out of the channel, fluidic tubing (silicon tubes) was attached to the slabs of the material. Typically holes are punched exactly at the three ends of E-shaped channel design. Silicon tubing was glued to the inlets and outlet by epoxy resin (Fig. 3).
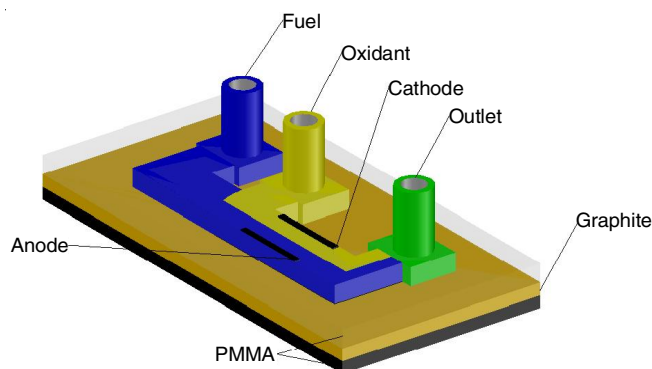
Fig. 3. Schematic diagram of the E-shaped membraneless laminar flow-based fuel cell with graphite plates molded with poly(dimethylsiloxane) (PDMS) and sealed with poly(methyl methacrylate) (PMMA)

Testing of fuel cell: The assembled fuel cells were tested in a configuration of alkaline and acid media (alkaline fuel and acidic oxidant). When the reactants were injected through the inlets, the fuel and the oxidant solutions merge at the E-junction (Fig. 4) and continue to flow in a laminar fashion in parallel over the anode and the cathode where both fuel and oxidant, respectively are oxidized and reduced. Polarization curves were obtained at different cell potentials using CS310 computer-controlled potentiostat with the associated Thales Z software package.

Potentiostat leads were attached to anodic and cathodic graphite current collectors using copper alligator clips. The lead of the working electrode was attached to anode while the reference and counter electrode leads were combined and attached to cathode. The potentiostat was used to generate an applied
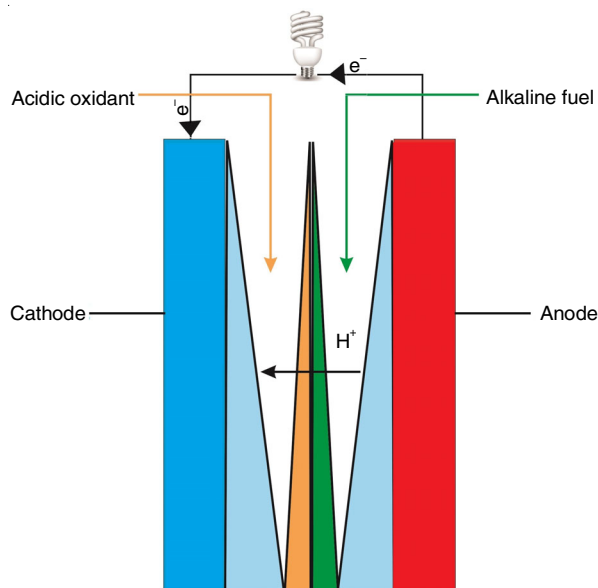
Fig. 4. Schematic diagram of the membraneless laminar flow-based fuel cell. The regions of fuel/oxidant depletion as well as regions of diffusional fuel crossover are indicated

potential and a multimeter (Fluke), with its leads attached to the anodic and cathode graphite current collectors was used to determine the actual cell potential.

The fuel and oxidant stream flow rates varied between 0.1 and 1.0 mL min^{-1} (per stream) using a syringe pump. Upon exiting each fuel cell, the streams travel through silicon tubing and get collected in a beaker. All the experiments were performed at room temperature.

RESULTS AND DISCUSSION

In this study, we treated membraneless formic acid fuel cell (MLFAFC) in all-acidic media, all-alkaline media, acid-alkaline media 1 (acidic anode and alkaline cathode), as well as alkaline-acid media 2 (alkaline anode and acidic cathode). For MLFAFCs, the anode stream had 0.15 M formic acid in 3.0 M NaOH and the cathode stream had 0.15 M percarbonate in 1.5 M H_2SO_4.

Performance of MLFAFC in all-acidic media: Eqns. 2 and 3 show the half-cell reactions and standard electrode potentials of formic acid oxidation and percarbonate reduction in acidic media. Eqn. 4 represents the overall cell reaction [9]. The acidic-acidic (both anode and cathode are acidic media) configuration provides a maximum theoretical open circuit potential (OCP) of 1.56 V. But we achieved the maximum potential 0.68 V at a current density of 14.03 mA cm^{-2} using our membraneless formic acid fuel cell:

Anode:
$$HCOOH \rightarrow CO_2 + 2H^+ + 2e^- \quad E° = 0.22 \text{ V} \quad (2)$$

Cathode:
$$3H_2O_2 + 6H^+ + 6e^- \rightarrow 6H_2O \quad E° = 1.78 \text{ V} \quad (3)$$

Overall:
$$HCOOH + 3H_2O_2 + 4H^+ + 4e^- \rightarrow CO_2 + 6H_2O \quad E° = 1.56 \text{ V} \quad (4)$$
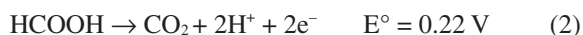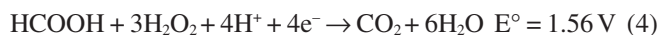
Performance of MLFAFC in all-alkaline media: The redox reactions and standard electrode potentials of formic

acid oxidation and percarbonate reduction in the alkaline media are shown in eqns. 5 and 6. Eqn. 7 represents the net cell reaction [10]. The all-alkaline configuration gives a maximum theoretical OCP of 2.156 V.

Anode:
$$2HCOO^- + 6OH^- \rightarrow 2CO_3^{2-} + 4H_2O + 4e^- \quad E° = -1.17 \text{ V} \quad (5)$$

Cathode:
$$3H_2O_2 + 6e^- \rightarrow 6OH^- \quad E° = 0.986 \text{ V} \quad (6)$$

Overall:
$$2HCOO^- + 3H_2O_2 + 2e^- \rightarrow 2CO_3^{2-} + 4H_2O \quad E° = 2.156 \text{ V} \quad (7)$$
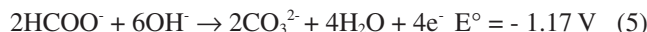
The mass transport limitations region, however, is reached at 1.08 V when 25.02 mA cm^{-2} of current density is achieved in the MLFAFC operating in an all-alkaline media.

Performance of MLFAFC in acidic-alkaline media 1 (acidic anode, alkaline cathode): In acidic-alkaline media system 1, one stream is acidic while the other stream is alkaline. In this configuration, the overall cell reaction (eqn. 8) can be obtained from eqns. 2 and 6. The maximum theoretical OCP obtained is 0.766 V in alkaline cathode and acidic anode configuration. An OCP of 0.415 V is observed as a result of over potentials on cathode and anode. This MLFAFC run in the acidic anode and alkaline cathode configuration is still limited by formic acid oxidation with the formation of CO intermediate in the presence of an acid, which causes a drop in the anode potential [11,12].

Anode:
$$HCOOH \rightarrow CO_2 + 2H^+ + 2e^- \quad E° = 0.22 \text{ V} \quad (2)$$

Cathode:
$$H_2O_2 + 2e^- \rightarrow 2OH^- \quad E° = 0.986 \text{ V} \quad (6)$$

Overall:
$$HCOOH + 3H_2O_2 \rightarrow CO_2 + 2H^+ + 2OH^- \quad E° = 0.766 \text{ V} \quad (8)$$
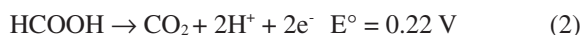
Performance of MLFAFC in alkaline-acid media 2 (acidic cathode, alkaline anode): In contrast, in alkaline anode and acidic cathode configuration, use of an alkaline fuel stream (eqn. 5) and an acidic oxidant stream (eqn. 3) allows energy to be obtained both from borohydride oxidation and percarbonate reduction reactions, as evident from the overall cell reaction (eqn. 9). The coupling of two galvanic reactions in this configuration yields a desirable high theoretical OCP of 2.95 V compared to H_2/O_2 and CH_3OH/O_2 fuel cells that provide equilibrium voltages of 1.23 and 1.20 V, respectively [13].

Anode:
$$HCOO^- + 3OH^- ! CO_3^{2-} + 2H_2O + 2e^- \quad E° = -1.17 \text{ V} \quad (5)$$

Cathode:
$$3H_2O_2 + 6H^+ + 6e^- \rightarrow 6H_2O \quad E° = 1.78 \text{ V} \quad (3)$$

Overall:
$$HCOO^- + 3H_2O_2 + 6H^+ + 3OH^- + 4e^- \rightarrow CO_3^{2-} + 8H_2O$$
$$E° = 2.95 \text{ V} \quad (9)$$

The use of alkaline anode and acidic cathode (alkaline-acid media 2) resulted in a higher overall cell potential than those obtained for all-alkaline, all acidic, alkaline-acid media 1 experiments in MLFAFC. For example, acid-alkaline media 2 yields a potential of 1.88 V, whereas both all-acidic, alkaline-

acid media 1 cells already start from a lower OCP and thus have a current density that are significantly lower than those of the alkaline-acid media 2.

At first look, the higher power densities of alkaline and acid media configuration 2 fuel cells may look very promising. Due to the higher power densities and higher cell potential, MLFAFC in alkaline-acid configuration 2 is subjected to further tests, such as ascertaining the effect of varying fuel and oxidant concentrations, flow rate variations, electrode distance effect, and cell stability test.

Influence of fuel concentration: On increasing the concentration of formic acid, fuel diffusion and the oxidation kinetics are observed to be improved, which leads to higher power density. However, formation of CO intermediate also increases, resulting in a decrease of open circuit voltage in turn. Therefore, the concentration of HCOOH has to be optimized for better cell performance. The effect of formic acid concentration on the performance of MLFAFC is studied by varying HCOOH concentration between 0.50 and 2.0 M in 3 M NaOH.

The cell polarization and power density curves are shown in Fig. 5. As HCOOH concentration changes, the cell OCP remains practically in the range 1.38-1.89 V and the current density varies between 67.35 and 56.55 mA cm^{-2} for 1.50 M HCOOH.
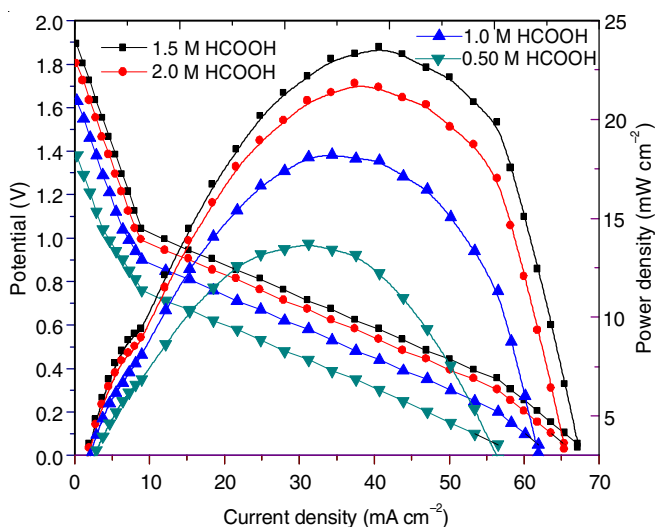
Fig. 5. Curves of cell polarization and power density for MLFAFC at different fuel concentrations: Fuel: X M in 3 M NaOH. Oxidant: 0.15 M percarbonate in 1.5 M H$_2$SO$_4$ solution. Flow rate of the reactants: 0.3 mL min^{-1}

Effect of oxidant composition: With liquid cathode reactant, rising percarbonate concentration leads to an increase in potential according to electrode reaction. Fig. 6 shows the influence of percarbonate concentration on the performance of MLFAFC. The cell voltage-current density polarization are completely different from Fig. 3, *i.e.* nearly linear decreasing of cell potential with an increase in current density. The cell performance improves on increasing percarbonate concentration from 0.050 to 0.15 M in 1.5 M H$_2$SO$_4$. However, further increase in percarbonate concentration leads to no change in cell performance. The peak power density is as high as 23.60 mW cm^{-2} at 0.57 V and 40.70 mA cm^{-2} for 0.150 M percarbonate, which is comparable to the air-breathing direct methanol fuel cell and much higher compared to membraneless microfuel cells of other designs [14].
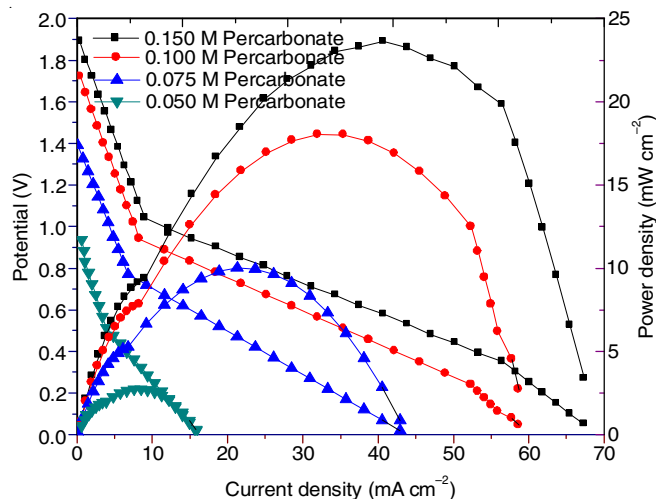
Fig. 6. Curves of cell polarization and power density of MLFAFC at different oxidant concentrations. Oxidant: X M percarbonate in 1.5 M H$_2$SO$_4$. Fuel: 1.50 M HCOOH in 3 M NaOH solutions. Flow rate of the reactants: 0.3 mL min^{-1}

Variation of electrolyte concentrations: The performance of oxidant is dependent on the electrolyte concentration. Fig. 7 shows that the power density of fuel cell increases when H$_2$SO$_4$ concentration increases from 0.10 to 1.50 M. When sulphuric acid concentration is increased further, the cell performance decreases. Therefore, 1.50 M H$_2$SO$_4$ is fixed as the ideal oxidant solution to be used as electrolyte.
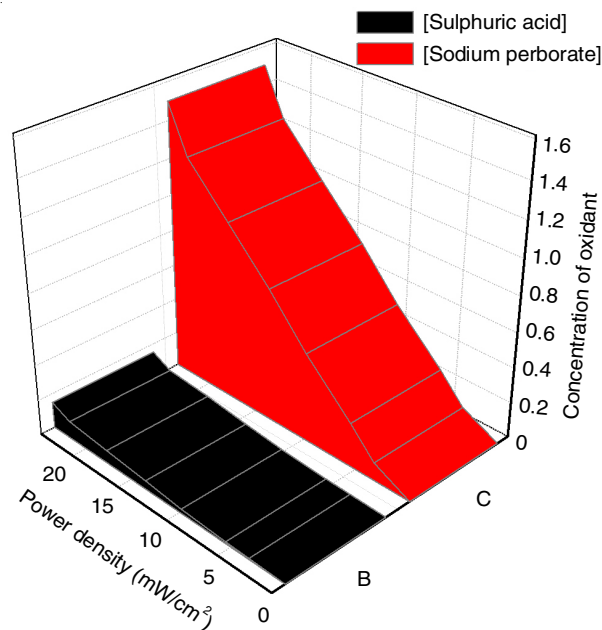
Fig. 7. Effect of various combinations of percarbonate and sulphuric acid concentrations on the maximum power density (23.60 mW cm^{-2}) of the MLFAFC at room temperature. The fuel mixture for variation of oxidant is ([fuel]: 1.5 M formic acid + 3 M NaOH, [oxidant]: X M percarbonate + 1.5 M H$_2$SO$_4$) and the fuel mixture for variation of sulphuric acid is ([fuel]: 1.50 M formic acid + 3 M NaOH, [oxidant]: 0.15 M percarbonate + x M H$_2$SO$_4$). Stream flow rates: 0.3 mL min^{-1}

The concentration of alkaline anolyte also affects the fuel cell performance. Increasing NaOH concentration upto 3 M has been found to be beneficial for MLFAFC performance in terms of enhanced OCP, power density and sustained current

density. Beyond NaOH concentration of 3 M, a negative effect is observed. Increasing concentration of NaOH manifests in negative effects of improving anode reaction, increasing the conductivity of NaOH solution [15]. Yet, increased NaOH concentration provides a negative effect to the cathode reaction and also leads to an increase in the solution viscosity, which decreases the movement of hydride ion in the catalyst layer [16].

Effect of flow rate: The effect of fuel mixture flow plays an important role in the performance of MLFAFCs and provides control over the carrying time of reacting species moving between the anode and the cathode. In this experiment, fuel mixture flow rates of 0.1, 0.2, 0.3, 0.4, 0.5, 0.6, 0.7, 0.8, 0.9 and 1.0 mL/min were tested. The cell potential and current density were considered with different external loads as a function of the flow velocity of the fuel mixture. Using the flow rate applied and the cross-sectional area of channel, flow velocity can be calculated. The higher potential and current density was found to be achieved at a flow rate of 0.3 mL flow rate, beyond which the cell performance is found to decrease as shown in Fig. 8.
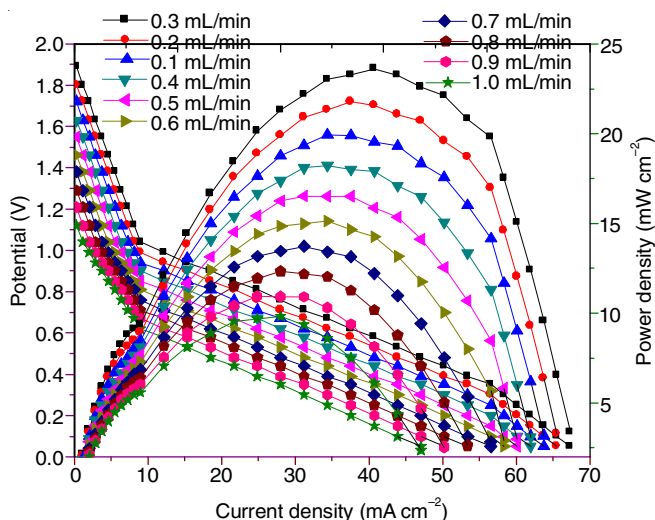
Fig. 8.   Curves of cell polarization and power density for MLFAFC at different flow rates. Fuel: 1.50 M HCOOH in 3 M NaOH solutions. Oxidant: 0.15 M percarbonate in 1.50 M H_2SO_4 solutions

Effect of distance between anode and cathode: The effect of distance between anode and cathode on the fuel cell output was experimentally studied. As different inter-electrode distances can significantly alter cell resistance and thus cell performance. The distance between anode and cathode varied from 1 to 100 mm. As the distance between anode and cathode is decreased, the maximum output power increased due to the reduced cell resistance. Fig. 9 shows that the maximum power density is achieved at an inter-electrode distance of 2 mm. Considering the role of a charge carrier, a shorter diffusion length is believed to lead to a faster electrochemical reaction because the diffusion time of reacting species would be shorter. Therefore, more reactions can take place at a given time, which increases the total number of charges involving the electrochemical reactions at the anode and cathode. This observation provides a clear evidence for the presence of a charge carrier moving between anode and cathode in the fuel mixture to complete the redox reactions of fuel cell [17].
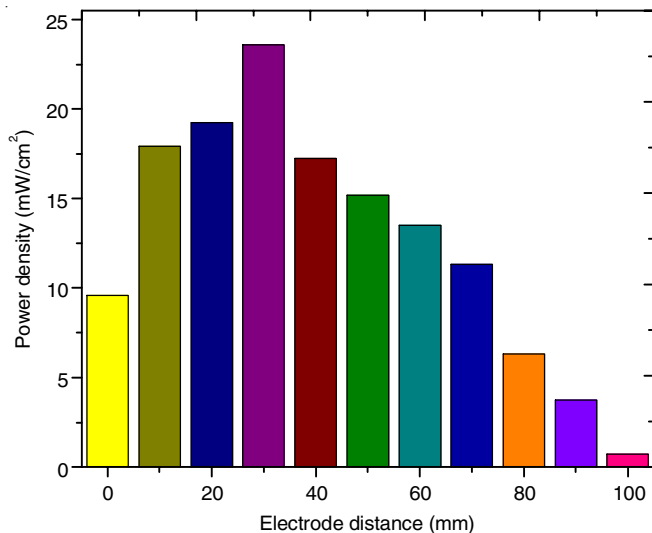
Fig. 9.   Effect of distance between the anode and the cathode on the maximum power density of the MLFAFC at room temperature. [Fuel]: 1.50 M formic acid + 3 M NaOH. [Oxidant]: 0.15 M percarbonate + 1.50 M H_2SO_4. Stream flow rates: 0.3 mL min^{-1}

Cell stability study: The stability of fuel cell was tested by applying a constant current density (30 mA cm^{-2}) in the absence of current flow. Short-term stability of MLFAFC was tested by monitoring the cell voltage change during the galvanostatic discharge of MLFAFC for a period of about 100 h (Fig. 10). The fluctuation in the cell voltage is due to addition of the solutions or restarting the experiments after an overnight break. The MLFAFC was found to maintain a relatively stable performance with little decay of cell voltage over the entire test period. The cause for deterioration is presumably because of the changes in the catalyst surface area, supplies of fuel and oxidant as well as the removal of product among others.
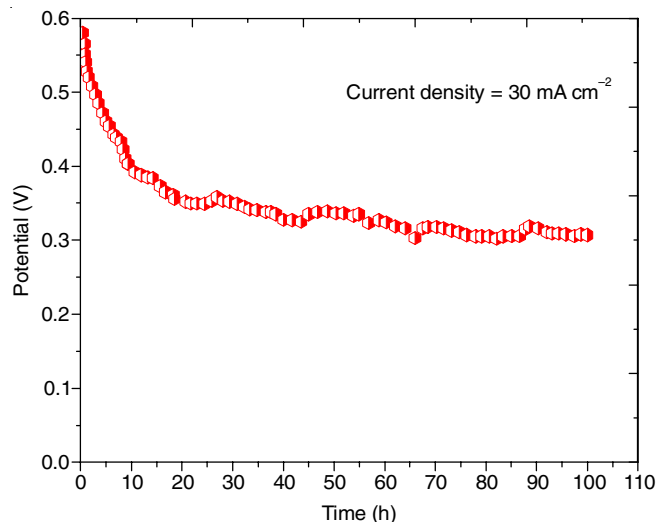
Fig. 10. Performance stability of the MLFAFC operating at a current density of 30 mA cm^{-2} at room temperature. [Fuel]: 1.50 M formic acid + 3 M NaOH. [Oxidant]: 0.15 M percarbonate + 1.5 M H_2SO_4. Stream flow rates: 0.3 mL min^{-1}

Conclusion

A membraneless formic acid fuel cell (MLFAFC) was made-up of poly(dimethylsiloxane) and its activity was analyzed under different operating conditions. Standard microfabrication

techniques were used to enlarge the fuel cell system. In this membraneless fuel cell, formic acid was used as a fuel at the anode and percarbonate was used as an oxidant at the cathode. The experiments described in this study indicate clearly that membraneless formic acid fuel cells are media flexible; they can operate in all-acidic, all-alkaline or even combined alkaline and acid media configurations. At room temperature, the laminar flow-based microfluidic fuel cell produced a maximum power density of 23.60 mW cm^{-2}. In the fuel cell, power density was found to increase with an increase in percarbonate concentration till 0.15 M and above this concentration, a decrease in cell performance was noted. The variation of formic acid concentration at the anode produced was found to have little influence on the cell performance. Thus, the present experimental results have confirmed that this membraneless microfuel cell is cathode-limited and indicate that a crucial factor for improving cell performance is increasing the concentration of oxidant in the cathode stream. The membraneless microfuel cell system investigated in this study seems to be a good candidate for feasible application in portable power electronics, because its performance is comparable to an air-breathing direct methanol fuel cell (DMFC). In addition, with varying flow rates, studying the effect of electrode distance and performing a durability test in present study, it is found that a flow rate of 0.3 mL and a distance of 30 mm distance results in good cell performance. Therefore, we expect that membraneless formic acid fuel cell may be a promising candidate for use as practical fuel cells to provide a clean and sustainable energy in future.

CONFLICT OF INTEREST

The authors declare that there is no conflict of interests regarding the publication of this article.

REFERENCES

1. S.A. Mousavi-Shaegh, N.-T.S.H. Nguyen, S.H. Chan and W. Zhou, *Int. J. Hydrogen Energy*, **37**, 3466 (2012); https://doi.org/10.1016/j.ijhydene.2011.11.051.

2. S.F.J. Flipsen, *J. Power Sources*, **162**, 927 (2006); https://doi.org/10.1016/j.jpowsour.2005.07.007.

3. E. Kjeang, N. Djilali and D. Sinton, *J. Power Sources*, **186**, 353 (2009); https://doi.org/10.1016/j.jpowsour.2008.10.011.

4. J. de Jong, R.G.H. Lammertink and M. Wessling, *Lab Chip*, **6**, 1125 (2006); https://doi.org/10.1039/b603275c.

5. A. Li, S.H. Chan and N.T. Nguyen, *Sustain. J. Micromechan. Microeng.*, **17**, 1107 (2007); https://doi.org/10.1088/0960-1317/17/6/002.

6. U.B. Demirci, *J. Power Sources*, **169**, 239 (2007); https://doi.org/10.1016/j.jpowsour.2007.03.050.

7. C.-F. Flores-River, *ISRN Applied Math.*, **2012**, Article 695167 (2012); https://doi.org/10.5402/2012/695167.

8. F.A. Cotton and G. Wilkilson, Advanced Inorganic Chemistry, Wiley Interscience: New York (1988).

9. C. Karunakaran and R. Kamalam, *J. Org. Chem.*, **67**, 1118 (2002); https://doi.org/10.1021/jo0158433.

10. M. Gowdhamamoorthi, A. Arun, S. Kiruthika and B. Muthukumaran, *J. Materials*, **2013**, Article 5480267 (2013); https://doi.org/10.1155/2013/548026.

11. R.S. Jayashree, L. Gancs, E.R. Choban, A. Primak, D. Natarajan, L.J. Markoski and P.J.A. Kenis, *J. Am. Chem. Soc.*, **127**, 16758 (2005); https://doi.org/10.1021/ja054599k.

12. M.P. Maher, J. Pine, J. Wright and Y. Tai, *J. Neurosci. Methods*, **87**, 45 (1999); https://doi.org/10.1016/S0165-0270(98)00156-3.

13. K.B. Min, S. Tanaka and M. Esashi, *Electrochemistry (Tokyo Jpn.)*, **70**, 924 (2002).

14. J.D. Morse, A.F. Janlowski, R.T. Graff and J.P. Hayes, *J. Vac. Sci. Technol. A*, **18**, 2003 (2000); https://doi.org/10.1116/1.582462.

15. J.H. Wee, *J. Power Sources*, **161**, 1 (2006); https://doi.org/10.1016/j.jpowsour.2006.07.032.

16. E.G. Dow, R.R. Bessette, G.L. Seeback, C. Marsh-Orndorff, H. Meunier, J. VanZee and M.G. Medeiros, *J. Power Sources*, **65**, 207 (1997); https://doi.org/10.1016/S0378-7753(97)02474-9.

17. S.M. Mitrovski, L.C.C. Elliott and R.G. Nuzzo, *Langmuir*, **20**, 6974 (2004); https://doi.org/10.1021/la048417w.